Modeling of $1/f$ Noise with HiSIM for 100nm CMOS Technology

Representative Hiroaki Ueno (Res. Asso. Graduate School of Advanced Sciences of Matter)
Cooperator Mitiko Miura-Mattausch (Prof., Graduate School of Advanced Sciences of Matter)

Abstract

A new $1/f$ noise model of MOSFETs for circuit simulation valid down to 100nm technology has been developed. The main feature of the model is inclusion of the carrier density distribution along the channel. The model is implemented into the circuit simulation model HiSIM based on the drift-diffusion approximation. It was proved that only one gate-length-independent model-parameter, the trap density, is sufficient to reproduce all measured $1/f$ noise characteristics.

1 Introduction

Accurate prediction of $1/f$ noise characteristics is becoming increasingly important for RF applications of MOSFETs, because the low-frequency $1/f$ noise affects for example the high frequency phase noise through upconversion [1].

The origin of the conventional $1/f$ noise in MOSFETs has been explained theoretically by a fluctuation in the number of channel carriers by trapping/detrapping processes at the oxide interface [2] and by a fluctuation in mobility [3]. However, shortcomings of existing $1/f$ noise models for circuit simulations are that they can hardly reproduce the strong gate length (L_g) dependence as well as the complicated bias dependence with a single model equation. The measured $1/f$ noise was found to exhibit the large increase of noise by reducing the gate length, which is stronger channel length dependence than predicted by the conventional $1/LW$ linear relationship [4].

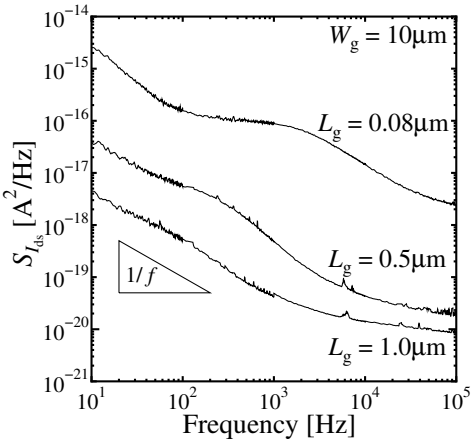

Fig. 1: Drain current noise of n-MOSFET with different gate length (0.08, 0.5 and 1.0μm) under linear condition.

Thus, our objective is to develop the $1/f$ noise model for circuit simulation valid for all gate lengths with a single parameter set. The model will be demonstrated to meet required accuracy for any bias conditions and gate lengths with a single model parameter set.

2 Analysis of Measured $1/f$ Noise Characteristics

The $1/f$ noise spectrum is obtained by assuming uniform trap density and energy distribution in the oxide layer [2]. However, as device size reduces, measured low-frequency noise strongly departs from the $1/f$ dependence as shown in Fig. 1. This means that the trap density and energy distribution is spatially non-uniform in the oxide layer [5, 6]

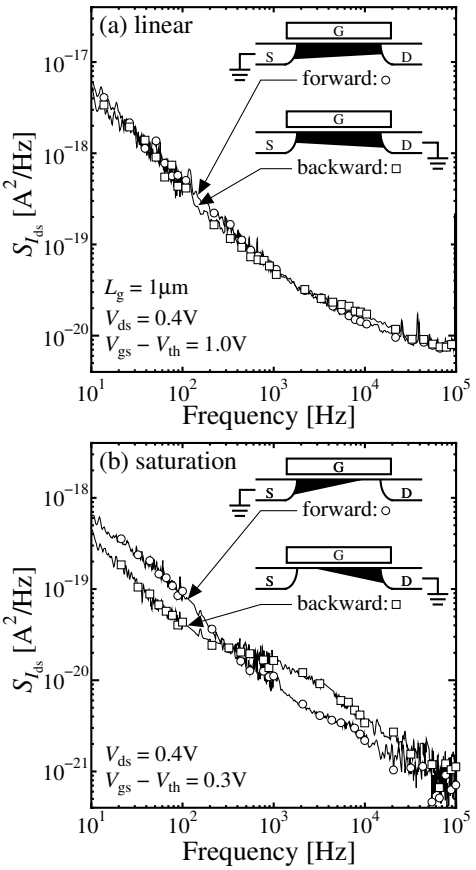

Fig. 2: Comparison of drain current noise spectrum density between forward measurement and backward measurement under (a) linear and (b) saturation condition for L_g = 1.0μm. The insets show schematics of the inversion charge distribution in the forward and backward measurement.

especially in smaller scale devices [7, 8]. Thus, the spatial distribution of the trap density determines the noise feature.

Figs. 2a and 2b show measured noise spectra under the linear and saturation conditions, respectively, for a gate length (L_g) of 1.0μm. The measurements with exchanged source (forward) and drain (backward) contacts are compared in the figures. The carrier density distribution along the channel is schematically depicted for each condition. Under the linear condition the difference in the noise spectra between the forward and backward measurement is hardly observed. On the contrary, the difference becomes clear under the saturation

condition. However, no difference in the measured drain current is observed by the exchange. This concludes that the measured characteristics in Figs. 2a and 2b are due to the position dependent trap density and energy along the channel direction, in which the drain current is insensitive.

The Lorentzian noise is described

$$S_{I_{ds}} = \frac{A\tau}{1 + (2\pi f\tau)^2} \tag{1}$$

where A is a magnitude of the Lorentzian noise determining the trap density, and τ is a time constant of the carriers in the generation-recombination process, determined by the position in the depth direction of the oxide layer [2, 9]. The calculation result with Eq. (1) is shown in Fig. 3 together with measurement [10]. Under the linear condition, the carrier concentration is rather homogeneous along the channel. Therefore, all trap sites along the channel causing the Lorentzian noise contribute on the noise characteristics for both the forward and backward cases, resulting in a nearly diminished difference in the measured noise spectra. On the contrary, the pinch-off condition occurs under the saturation condition, and the carrier distribution along the channel becomes inhomogeneous.

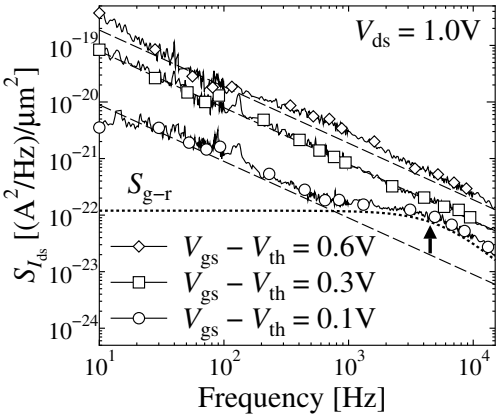

Fig. 3: Measured drain current noise power spectra $S_{I_{ds}}$ versus frequency for various $V_{gs} - V_{th}$ values. Three dashed lines represent ideal $1/f$ spectra and the dotted line is the result fitted with Eq. (1).

neous.

Figs. 4a and 4b show the same measurement as Figs. 2a and 2b but for $L_g = 0.12\mu$m case. The difference in the forward and backward noise measurements under the saturation condition is enhanced. The reason is that the contribution of each inhomogeneous trap site on the noise characteristics is enhanced due to the reduced gate length. There is again no distinguishable difference in the measured drain current identical for the forward and the backward measurement of the $L_g = 1.0\mu$m case.

The above investigation proved that the non-$1/f$ noise is due to the non-uniform trap density. Thus, by averaging the noise spectra over chips on a wafer, it is expected that the noise reduces to the $1/f$ characteristics [11]. Fig. 5 shows measured noise spectra of about 30 different chips on a wafer for $L_g = 0.46\mu$m at $f = 100$Hz. The average of all these

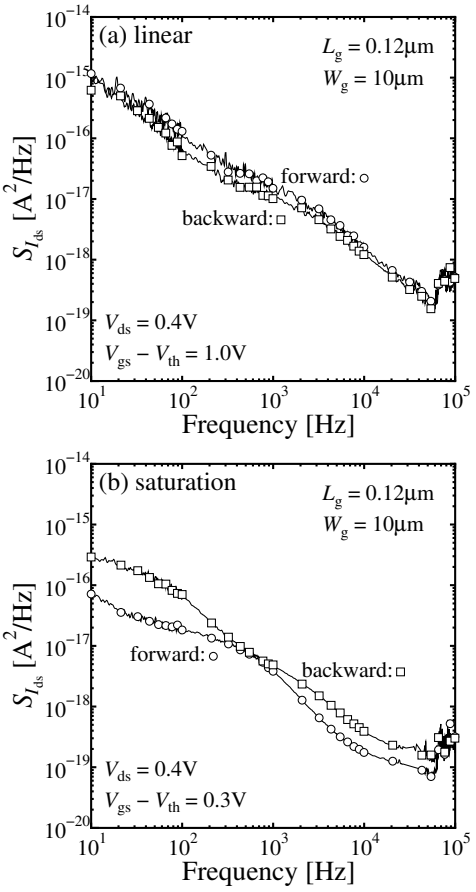

Fig. 4: Comparison of drain current noise spectrum density between forward measurement and backward measurement under (a) linear and (b) saturation condition for $L_g = 0.12\mu$m.

noise spectra exhibits really the $1/f$ noise characteristics as shown by a thick line. This concludes that trap sites causing the Lorentzian noise spectra distribute randomly on a wafer as can be seen from the Gaussian distribution of the noise spectrum density at $f = 100$Hz shown in Fig. 6. Thus as a circuit-simulation model it is a subject to describe only this averaged $1/f$ noise characteristics with boundaries as the worst and the best case.

3 Model Description

The general expression for the $1/f$ noise power spectrum density of a MOSFET ($S_{I_{ds}}$) [2, 12] has a position-integral part of the inversion-charge density ($N(x)$) along the channel direction x

$$S_{I_{ds}}(f) = \frac{I_{ds}^2 N_{trap} kT}{L^2 W q f} \int_0^L \left(\frac{1}{N(x) + N^*} \pm \alpha\mu \right)^2 \mathrm{d}x \tag{2}$$

$$N^* = \frac{kT}{q^2}(C_{ox} + C_{dep} + C_{it}) \tag{3}$$

where k is the Boltzmann constant, T is the lattice temperature, L is the channel length, W is the channel width, q is the electron charge, μ is the carrier mobility, C_{ox} is the gate oxide capacitance and C_{dep} is the depletion layer capacitance. The model parameters N_{trap} ($= N_t/\gamma$), α and C_{it} are the ratio

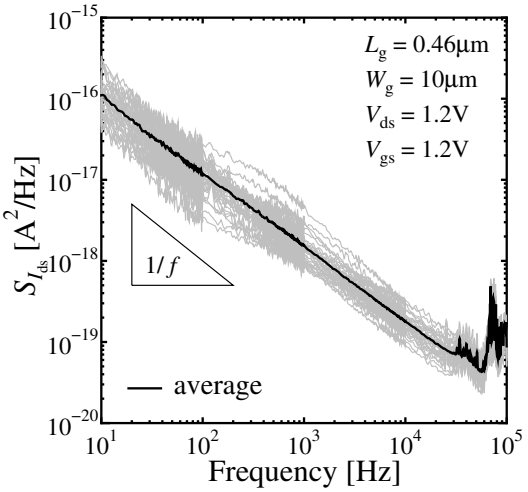

Fig. 5: Measured drain current noise spectra of about 30 devices with the same size under the same bias condition on a wafer. The fat curve represents an averaged noise spectrum.

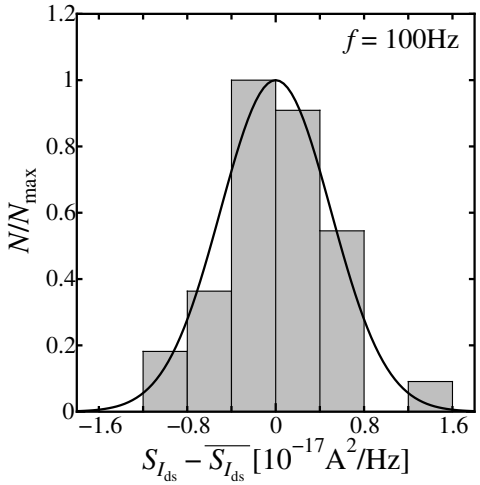

Fig. 6: Histogram of measured drain current noise spectra at 100Hz. The curve shows the normal distribution function. $\overline{S_{I_{ds}}}$ is about 1.0×10^{-17}A^2/Hz.

of trap density (N_t) to attenuation coefficient into the oxide γ, the contribution coefficient of the mobility fluctuation and the capacitance caused by the interface trapped carriers, respectively. To develop an precise $1/f$ noise model, therefore, not only the current I_{ds} itself, but also the position dependent carrier concentration along the channel $N(x)$ is necessary. Our new $1/f$ noise model is linked with the circuit simulation model HiSIM [13], based on the drift-diffusion approximation [14]. HiSIM provides the carrier concentrations at the source N_0 and drain side N_L determined by surface potentials consistently. Beyond the pinch-off point under the saturation condition the carrier concentration becomes negligibly small, thus the integration in Eq. (2) is done from ϕ_{s0} to ϕ_{sL}. Thus, our description of the $1/f$ noise spectrum density is

$$S_{I_{ds}}(f) = \frac{I_{ds}^2 N_{trap} kT}{L^2 W q f} \int_{\phi_{s0}}^{\phi_{sL}} \left(\frac{1}{N(\phi) + N^*} \pm \alpha v \right)^2 d\phi \quad (4)$$

In Eq. (4) the mobility μ is replaced by v of the second term in the parenthesis of the right-hand side of Eq. (2). The reason is that the field increase along the channel has to be considered together with the mobility distribution. In order to perform the integration analytically an assumption is applied. Namely, $N(x)$ is linearly decreasing from N_0 to N_L. This can be verified with two-dimensional simulation results with MEDICI [15] in Fig. 7. For the two-dimensional simulation the impurity profile was extracted by the inverse modeling from measured current-voltage characteristics. It is seen that the linear approximation of $N(x)$ is applicable for any bias conditions.

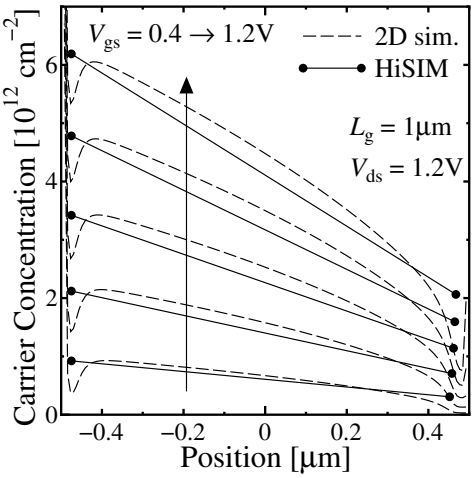

Fig. 7: The inversion-charge density at the source N_0 and drain side or pinch-off point in saturation condition N_L calculated by HiSIM. The position dependence of $N(x)$ calculated by two-dimensional device simulator is also depicted.

The validity of the exclusion of the channel region beyond the pinch-off point is proved here. In the pinch-off region carriers loose the gate voltage control and number of carriers reduces drastically. Thus, diminished trapping/detrapping process is expected due to diminished collision with the interface. Fig. 8 shows the simulated number of channel electrons colliding with the oxide interface per unit time by the Monte Carlo simulator FALCON [16] as a function of position along the channel [10]. The FALCON includes all scattering mechanisms important for MOSFETs with a full-energy-band structure. Thus, the diminished noise power arises from the pinch-off region and L in Eq. (2) can be replaced by $L - \Delta L$ where ΔL is the length of the pinch-off region [17].

The final analytical equation of the $1/f$ noise, valid for all bias conditions, is derived

$$S_{I_{ds}}(f) = \frac{I_{ds}^2 N_{trap} kT}{(L - \Delta L) W q f} \left\{ \frac{1}{(N_0 + N^*)(N_L + N^*)} + \frac{2\alpha v}{N_L - N_0} \log\left(\frac{N_L + N^*}{N_0 + N^*} \right) + (\alpha v)^2 \right\} \quad (5)$$

where N_{trap} is the model parameter, and N_0 and N_L are calculated by HiSIM.

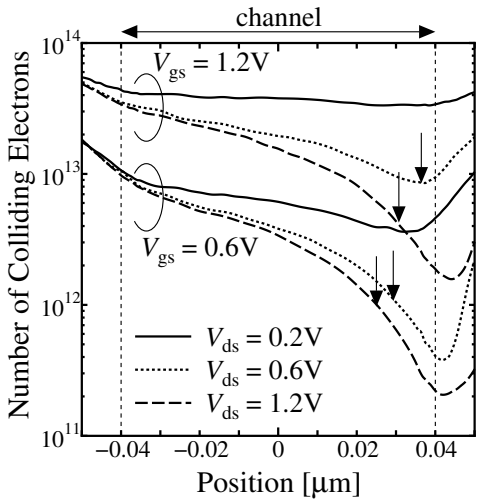

Fig. 8: Monte Carlo simulation result for number of electrons colliding with the oxide interface per unit time as a function of position along the channel for $L_g = 0.12\mu$m. The vertical arrows indicate pinch-off points.

4 Calculation Results

Fig. 9 shows the measured V_{gs} dependence of $S_{I_{ds}}$ of n-MOSFETs for different V_{ds} values with $L_g = 1.0$, 0.46 and 0.12μm at $f = 100$Hz by symbols. All measured points are average values over 30 samples on a wafer. Calculated results with our model are also shown by solid curves. It is seen that the bias dependences of the noise characteristics for all channel lengths are well reproduced with a single model-parameter set. Fig. 10 shows the measured V_{ds} dependence of $S_{I_{ds}}$ of n-MOSFETs for different V_{gs} values. Among three model parameters (N_{trap}, α, C_{it}), two parameters (α and C_{it}) were extracted to be negligibly small. And only L_g independent N_{trap} is responsible for the measured $1/f$ characteristics.

The dotted curves in Fig. 9 are calculated results with averaged $N(x)$ in the channel (N_{ave}) instead of the integration explicitly as shown below:

$$S_{I_{ds}}(f) = \frac{I_{ds}^2 N_{trap} kT}{(L-\Delta L)Wqf}\left\{\frac{1}{N_{ave}+N^*}+(\alpha v)\right\}^2 \qquad (6)$$

It is seen that the results with N_{ave} cannot reproduce the bias dependences of the $S_{I_{ds}}$ for all channel lengths with a single model-parameter set. Especially the noise enhancement for larger V_{ds} is not well reproduced. Thus, we can conclude that the position dependence of the carrier concentration plays an important role for the $1/f$ noise characteristics. For the successful prediction of the $1/f$ noise characteristics, the measured I–V characteristics have to be accurately simulated, since N_0 and N_L are important origin of the complicated bias dependent $1/f$ noise. To verify the role of our argument, we compare the V_{ds} dependence of the drain current noise (solid curves) and square of drain current (dotted curves) in Fig. 11. Roughly, the $1/f$ noise characteristics are governed by the I_{ds}^2 characteristics. However, clear deviations between two are observed. Especially, the $S_{I_{ds}}$–V_{ds} characteristics in linear condition are different from the I_{ds}–V_{ds} characteristics. In linear condition, terms of N_L cannot be negligible in Eq. (5). Thus, the bias dependence of the $1/f$ noise is due to not only the I–V characteristics but also the bias dependence of N_0 and N_L.

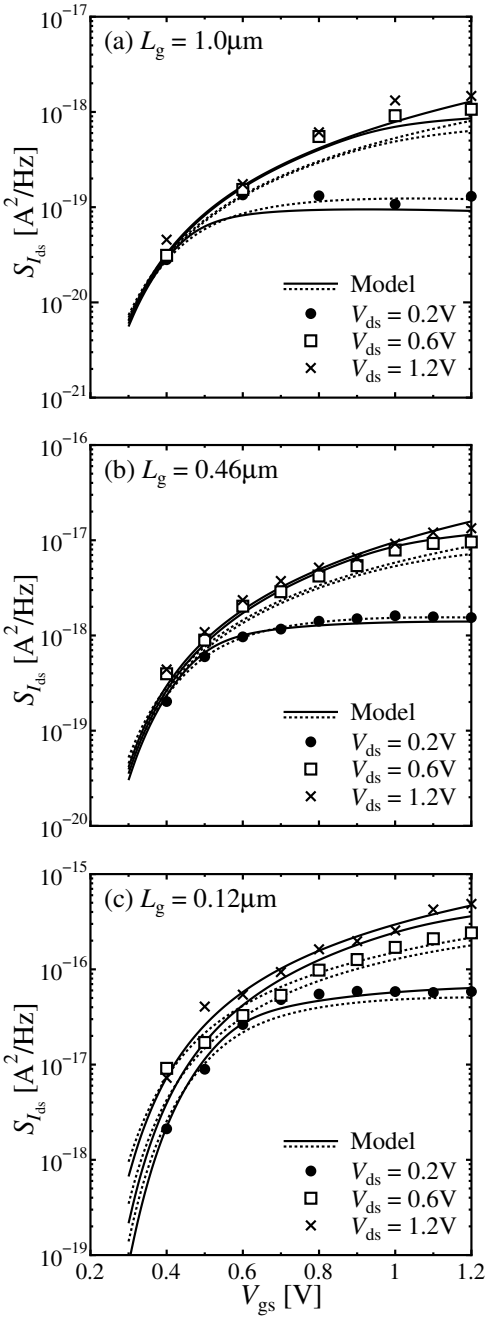

Fig. 9: Comparison of the V_{gs} dependence of the measured and simulated drain current noise by our model for (a) $L_g = 1.0\mu$m, (b) 0.46μm and (c) 0.12μm at frequency 100Hz. Model parameter values are the same for all L_g values. Dotted curves represent calculated results with N_{ave} instead of N_0 and N_L.

Fig. 12 shows the device area LW dependence of measured $S_{I_{ds}}$ normalized by I_{ds}^2 at $f = 100$Hz, where W_g is fixed to 10μm. The well-confirmed $1/LW$ dependence is still preserved for 100nm-MOSFETs. However, the deviation from the linear relationship is observed beyond $L_g = 0.14\mu$m. The

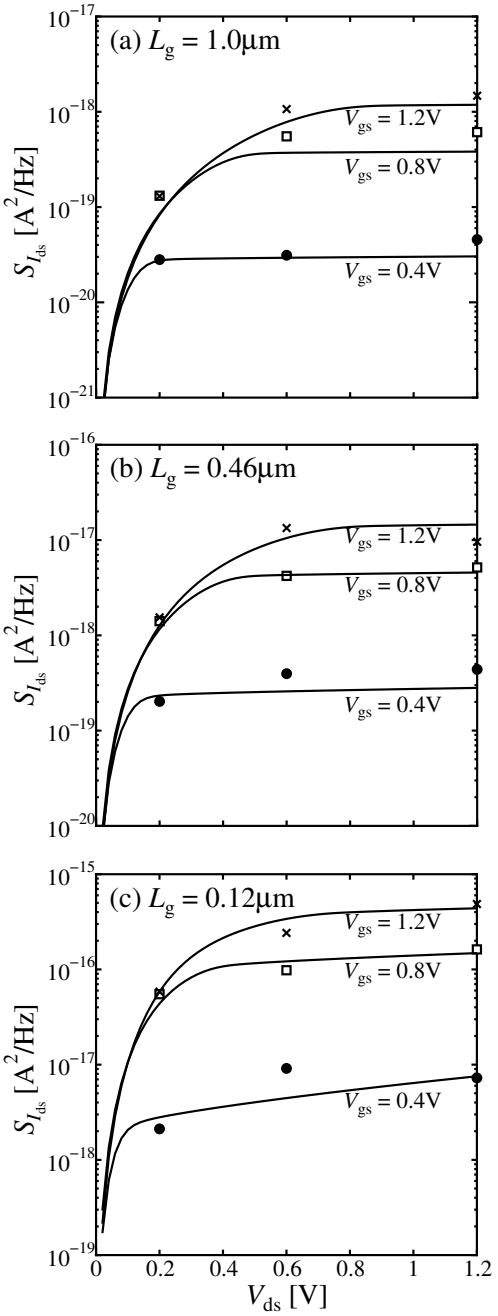

Fig. 10: Comparison of the V_{ds} dependence of the measured and simulated drain current noise by our model for (a) L_g = 1.0μm, (b) 0.46μm and (c) 0.12μm at frequency 100Hz.

enhancement is attributed to the high-field effects becoming more pronounced for smaller L_g. It is seen in Fig. 9 that the present model is valid even for such case.

5 Conclusion

We have demonstrated that the non-$1/f$ noise characteristic is caused the inhomogeneous trap density distribution along the channel. Averaged noise spectra on a wafer reduces to the $1/f$ characteristic, which is suitable for the modeling. A new $1/f$ noise model for circuit simulation based on the drift-diffusion approximation, reproduces the bias and L_g dependence of the averaged noise spectrum with only three model parameters. Practically only one model parameter is responsible for describing the measured $1/f$ characteristics.

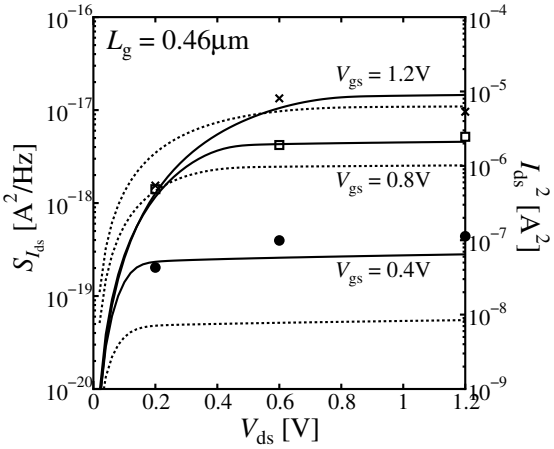

Fig. 11: Comparison of the V_{ds} dependence of the measured and simulated drain current noise (solid curves) and square of drain current (dotted curves).

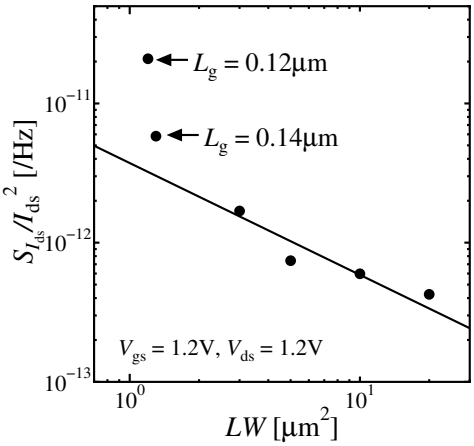

Fig. 12: Measured drain current noise power spectrum density $S_{I_{ds}}$ normalized by I_{ds}^2 vs. gate area LW. The solid line is the $1/LW$ linear relationship.

References

[1] A. Hajimiri and T. H. Lee, "A general theory of phase noise in electrical oscillators," *IEEE J. Solid-State Circ.*, **33**, 179, 1998.

[2] S. Christensson, I. Lundstrom, and C. Svensson, "Low frequency noise in MOS transistors — I: theory," *Solid-State Electron.*, **11**, 797, 1968.

[3] F. N. Hooge, "$1/f$ noise sources," *IEEE Trans. Electron Devices*, **41**, 1926, 1994.

[4] M. Tsai and T. Ma, "The impact of device scaling on the current fluctuations in MOSFETs," *IEEE Trans. Electron Devices*, **41**, 2061, 1994.

[5] M. J. Deen, M. E. Levinshtein, S. L. Rumyantsev, and J. Orchard-Webb, "Generation-recombination noise in MOSFETs," *Semicond. Sci. Technol.*, **14**, 298, 1999.

[6] A. A. Balandin, *Noise and Fluctuations Control in Electronic Devices*, (American Scientific Publishers, California, 2002), p. 201.

[7] A. Longoni, E. Gatti, and R. Sacco, "Trapping noise in semiconductor-device — A method for determining the noise spectrum as a function of the trap position," *J. Appl. Phys.*, **78**, 6283, 1995.

[8] R. Brederlow, W. Weber, D. Schmitt-Landsiedel, and R. Thewes, "Fluctuations of the low frequency noise of MOS transistors and their modeling in analog and RF-circuits," *Tech. Dig. of IEDM*, p. 159, 1999.

[9] C. Delseny, F. Pascal, S. Jarrix, G. Lecoy, J. Dangla, and C. Dubon-Chevallier, "Excess noise in AlGaAs/GaAs heterojunction bipolar-transistors and associated TLM test structures," *IEEE Trans. Electron Devices*, **41**, 2000, 1994.

[10] H. Ueno, T. Kitamura, S. Matsumoto, T. Okagaki, M. Miura-Mattausch, H. Abe, and T. Hamasaki, "Evidence for an additional noise source modifying conventional $1/f$ frequency dependence in sub-μm metal-oxide-semiconductor field-effect transistor," *Appl. Phys. Lett.*, **78**, 380, 2001.

[11] S. Matsumoto, H. Ueno, S. Hosokawa, M. Miura-Mattausch, H. J. Mattausch, S. Kumashiro, T. Yamaguchi, K. Yamashita, and N. Nakayama, submitted for publication.

[12] K. K. Hung, P. K. Ko, C. Hu and Y. C. Cheng, "A physics-based MOSFET noise model for circuit simulators," *IEEE Trans. Electron Devices*, **37**, 1323, 1990.

[13] M. Miura-Mattausch, H. Ueno, H. J. Mattausch, K. Morikawa, S. Itoh, A. Kobayashi, and H. Masuda, "100nm-MOSFET Model for Circuit Simulation: Challenges and Solutions," *IEICE Trans. Electron.*, **E86-C**, 1009, 2003.
HiSIM1.2.0 User's Manual, April 2003, http://www.starc.or.jp/kaihatu/pdgr/hisim/index.html

[14] M. Miura-Mattausch, U. Feldmann, A. Rahm, M. Bollu, and D. Savignac, "Unified complete MOSFET model for analysis of digital and analog circuits," *IEEE Trans. CAD/ICAS*, **15**, 1, 1996.; M. Miura-Mattausch, H. Ueno, M. Tanaka, H. J. Mattausch, S. Kumashiro, T. Yamaguchi, K. Yamashita, and N. Nakayama, "HiSIM: A MOSFET Model for Circuit Simulation Connecting Circuit Performance with Technology,"*Tech. Dig. of IEDM*, p. 109, 2002.

[15] *MEDICI User's Manual*, (Synopsys Co., 2002).

[16] C. Jungemann, S. Yamaguchi, and H. Goto, "On the accuracy and efficiency of substrate current calculation for sub-μm n-MOSFETs," *IEEE Electron Device Lett.*, **17**, 464, 1996.

[17] D. Navarro, T. Mizoguchi, M. Suetake, S. Ooshiro, K. Hisamitsu, H. Ueno, M. Miura-Mattausch, H. J. Mattausch, S. Kumashiro, T. Yamaguchi, K. Yamashita, and N. Nakayama, "Modeling of the pinch-off condition in 100nm-MOSFETs for circuit simulation based on the surface-potential description," submitted for publication.

6 Published Papers and Patents

Published Papers

1. M. Tanaka, H. Ueno, O. Matsushima, and M. Miura-Mattausch, "High-Electric-Field Electron Transport at Silicon/Silicon-Dioxide Interface Inversion Layer," Jpn. J. of Appl. Phys.," **42**, pp. L280–L282, (2003).

2. N. Nakayama, H. Ueno, T. Inoue, T. Isa, M. Tanaka, and M. Miura-Mattausch, "A Self-Consistent Non-Quasi-Static MOSFET Model for Circuit Simulation Based on Transient Carrier Response," Jpn. J. of Appl. Phys., **42**, pp. 2132–2136, (2003).

3. M. Miura-Mattausch, H. Ueno, H. J. Mattausch, K. Morikawa, S. Itoh, A. Kobayashi, and H. Masuda, "100nm-MOSFET Model for Circuit Simulation: Challenges and Solutions (Invited)," IEICE Transactions on Electronics, **E86-C**, pp. 1009–1021, (2003).

4. N. Nakayama, D. Navarro, M. Tanaka, H. Ueno, M. Miura-Mattausch, H. J. Mattausch, T. Ohguro, S. Kumashiro, M. Taguchi, T. Kage, and S. Miyamoto, "A Non-Quasi-Static Model for MOSFET Based on Carrier-Transit Delay," IEE Electronics Letters, *in print*.

5. S. Hosokawa, D. Navarro, H. Ueno, M. Miura-Mattausch, H. J. Mattausch, T. Ohguro, S. Kumashiro, M. Taguchi, T. Kage, and S. Miyamoto, "Universal Thermal-Drain-Noise Prediction from Threshold Voltage," IEEE Electron Device Letters, *in print*.

Proceedings

1. T. Mizoguchi, H. J. Mattausch, H. Ueno, D. Kitamaru, K. Hisamitsu, M. Miura-Mattausch, S. Itoh, and K. Morikawa, "Extraction of Inter- and Intra-Chip Device-Parameter Variations with a Differential-Amplifier-Stage Test Circuit," Workshop on Synthesis and System Integration of Mixed Information Technologies, (2003).

2. O. Matsushima, M. Tanaka, H. Ueno, K. Hara, K. Konno, and M. Miura-Mattausch, "Carrier Transport in Highly Generated Carrier Concentration," 13th International Conference on Nonequilibrium Carrier Dynamics in Semiconductors, (2003).

3. S. Hosokawa, Y. Shiraga, H. Ueno, M. Miura-Mattausch, H. J. Mattausch, T. Ohguro, S. Kumashiro, M. Taguchi, H. Masuda, and S. Miyamoto, "Investigation of Enhanced Thermal Noise for 100nm-MOSFETs," International Conference on Solid State Devices and Materials, (2003).